MOVEMENT DETECTION USING A RECIPROCAL RECEIVED SIGNAL STRENGTH MODEL

Ossi Kaltiokallio[†] *Hüseyin Yiğitler*[⋆]

[†] Information Technology and Communication Sciences, Tampere University, Finland
[⋆] Department of Communications and Networking, Aalto University, Finland
Emails: ossi.kaltiokallio@tuni.fi, huseyin.yigitler@aalto.fi

ABSTRACT

Received signal strength measurements of commodity radios can be utilized for sensing the surrounding environment. This work harnesses the signal strength measurements for estimating time periods when a person is stationary and moving. A novel reciprocal signal strength model is presented, and an energy detector is developed. It is shown that the decision threshold can be calculated in closed form for the proposed model. In addition, the observation time window can be minimized to one communication cycle which equals 58 milliseconds in our case. Using real-world experimental data from two different environments, it is demonstrated that movement can be correctly detected over 99% of the time.

***Index Terms*—** Movement detection, energy detector, received signal strength, reciprocal channel

1. INTRODUCTION

The radio of commodity wireless devices, provided that it can measure the received signal strength, can be used to develop novel radio frequency (RF) sensing applications [1]. These applications leverage human-induced perturbations to propagation patterns of radio signals which causes a measurable change in the received signal. Since the changes in the measured signal are a function of the person's position, electrical properties and velocity [2], RF sensing enables a wide range of applications including but not limited to: localization [3], breathing monitoring [4], occupancy assessment [5] and crowd size estimation [6].

One of the pioneering works in RF sensing demonstrated that people alter the mean and variance of the signal strength [7] and it was shown that anomalies in the measurement statistics can be used to detect the presence of people [8]. Modeling the vacant and occupied states independently improves detection performance [9] and it also enables device-free localization [10, 11, 12]. The statistical model also depends on the number of people [3, 5], and the linear relationship between the number of people and average signal strength was used in [6] to estimate crowd sizes up to thousands of people. The aforementioned works rely on training for estimating the measurement statistics. Systems that do not require training and that can detect movement have been presented in [13, 14, 15]. However, the decision is made using data over a several second time window and precise movement detection is not possible.

In this work, an energy-based movement detector that utilizes a novel reciprocal signal strength model is presented. It is shown that the decision threshold can be calculated in closed form for the proposed model, as opposed to works in [7, 13, 14] that rely on ad hoc methods. The proposed reciprocal model also minimizes the used observation time window to one communication cycle. The achieved decision agility is a significant improvement compared with the related works, which typically use a data set acquired over tens of communication cycles [13].

2. ENERGY DETECTOR

In this paper, we are interested in detecting movement of a person using L observations $\mathbf{y} = [y_1, \ldots, y_L]^T$. This problem can be formulated as binary hypothesis testing in which the detector decides between the null hypothesis H_0 (no movement) and the alternate hypothesis H_1 (movement). Applying Bayes' criterion to the minimum probability error detector and assuming the priori probabilities are equal results in the following likelihood ratio test [16, sec. 5.2]

$$\frac{p\left(\mathbf{y}|H_1\right)}{p\left(\mathbf{y}|H_0\right)} \underset{H_0}{\overset{H_1}{\gtrless}} 1, \tag{1}$$

where $p(\cdot)$ denotes the likelihood. Let us assume that under hypothesis H_0 the observations are zero mean Gaussian with unequal variance $y_l \sim \mathcal{N}(0, \sigma^2_{l,0})$, while under hypothesis H_1 the observations are corrupted by additive noise so that $y_l \sim \mathcal{N}(0, \sigma^2_{l,1})$ and $\sigma^2_{l,1} > \sigma^2_{l,0}$. For L independent observations the likelihood under hypothesis i is $p\left(\mathbf{y}|H_i\right) = \prod_{l=1}^{L} \mathcal{N}(0, \sigma^2_{l,i})$. Plugging the likelihood into (1) and taking the logarithm yields

$$\sum_{l=1}^{L} \left(\frac{1}{\sigma^2_{l,0}} - \frac{1}{\sigma^2_{l,1}} \right) y_l^2 \underset{H_0}{\overset{H_1}{\gtrless}} \sum_{l=1}^{L} \log \left(\frac{\sigma^2_{l,1}}{\sigma^2_{l,0}} \right). \tag{2}$$

If it is further assumed that the measurements in each state are i.i.d., $\forall\sigma_{l,0}^2 = \sigma_0^2$ and $\forall\sigma_{l,1}^2 = \sigma_1^2$, Eq. (2) simplifies to

$$\sum_{l=1}^{L} y_l^2 \underset{H_0}{\overset{H_1}{\gtrless}} L \log\left(\frac{\sigma_1^2}{\sigma_0^2}\right) \frac{\sigma_0^2\sigma_1^2}{\sigma_1^2 - \sigma_0^2}. \tag{3}$$

The presented detectors use the Bayes' criterion which requires that the priori probabilities of the hypothesis are known and it is possible to assign costs to the decisions. However, it is very difficult to assign realistic costs and priori probabilities for the considered problem and therefore, the Neyman-Pearson criterion is better suited. This criterion requires that the probability of false alarm, P_f, is fixed to some value while the probability of detection, P_d, is maximized [16, sec. 5.4]. The distribution of the sufficient statistic is not tractable in Eq. (2) and the Neyman-Pearson criterion cannot be used with this signal model. On the other hand, the sufficient statistic, $\varepsilon \triangleq \sum_{l=1}^{L} y_l^2$, given in Eq. (3) has a known distribution and as a result, P_f and P_d can be derived in closed form. Now, ε is an L degrees of freedom chi-squared distributed random variable with density function [17, p.45]

$$f(\varepsilon) = \frac{1}{\left(2\sigma_i^2\right)^{L/2}\,\Gamma(L/2, 0)} \varepsilon^{\frac{L}{2}-1} \exp\left(-\frac{\varepsilon}{2\sigma_i^2}\right) \tag{4}$$

where $\Gamma(\cdot,\cdot)$ is the upper incomplete gamma function [18, sec. 6.5]. Let $f_{\varepsilon|H_0}(x|H_0)$ denote the conditional density of ε under hypothesis H_0, then the probability of false alarm, $P_f \triangleq \Pr[\varepsilon > \gamma|H_0]$, is

$$P_f = \int_{\gamma}^{\infty} f_{\varepsilon|H_0}(x|H_0)\,dx = \Gamma\left(\frac{L}{2}, \frac{\gamma}{2\sigma_0^2}\right), \tag{5}$$

where $\Gamma(\cdot)$ is the regularized upper incomplete gamma function. Since $\Gamma(\cdot)$ has an inverse, the decision threshold can be determined from P_f using

$$\gamma = 2\sigma_0^2 \left[\Gamma\left(\frac{L}{2}, P_f\right)\right]^{-1}. \tag{6}$$

Similarly, we can derive an expression for the probability of detection, $P_d \triangleq \Pr[\varepsilon > \gamma|H_1]$, given by

$$P_d = \Gamma\left(\frac{L}{2}, \frac{\gamma}{2\sigma_1^2}\right) = \Gamma\left(\frac{L}{2}, \frac{\sigma_0^2}{\sigma_1^2}\left[\Gamma\left(\frac{L}{2}, P_f\right)\right]^{-1}\right). \tag{7}$$

In this paper, we consider two detectors with different signal models and decision criterion. The first is an energy detector with unequal variance (EDUV), which is the likelihood ratio test given in Eq. (2), and it uses the Bayes' criterion. The second is an energy detector with equal variance (EDEV) in Eq. (3) and it uses the Neyman-Pearson criterion. Despite their differences, operation of the detectors are the same; they calculate the sufficient statistic, ε, and make a decision based on a threshold, γ, associated with the decision criteria.

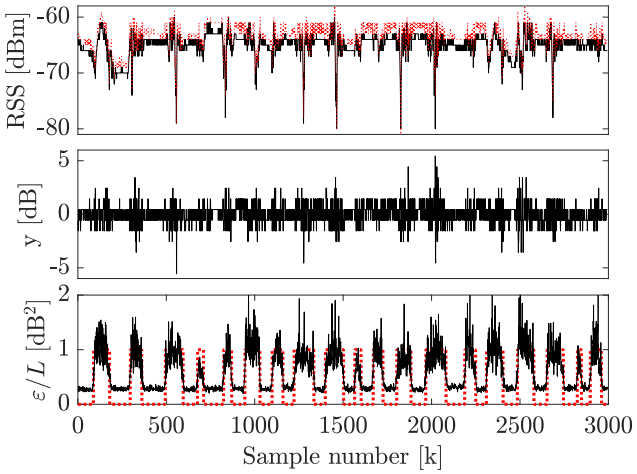

Fig. 1: Energy detector example. On top, signal strength in both directions of a reciprocal link and in the middle, $y_l(k)$. On the bottom, the normalized sufficient statistic (—) and movement indicator (·····), 0 for H_0 and 1 for H_1.

3. RECIPROCAL OBSERVATION MODEL

This section introduces the observation model of the energy detector and methods to estimate parameters of the model. Let us consider link l that consists of nodes i and j, and time window $\mathcal{T} = \{t \mid (k-1)\,T < t \leq k\,T\}$ in which k denotes the sample number and T duration of the time window. At time $t_a \in \mathcal{T}$, node i transmits and the signal strength measured at node j is $r_{ij}(t_a)$. Correspondingly, node j transmits at time $t_b \in \mathcal{T}$ and the signal strength measured at node i is $r_{ji}(t_b)$. The difference in signal strength is

$$y_l(k) = \Delta r_l(k) - \mu_l + n(k) \tag{8}$$

where $\Delta r_l(k) = r_{ij}(t_a) - r_{ji}(t_b)$, μ_l is an offset between r_{ij} and r_{ji} and n is zero-mean Gaussian measurement noise with variance $\sigma_{l,0}^2$.

In a reciprocal channel, the channel gains are identical in both directions. Although the radio channel is reciprocal, measurements of the radio channel are not reciprocal for three reasons. First of all, additive noise contributes to each measurement randomly. Second, the hardware used by the transceivers are not identical and the hardware induced effects are different in each direction. As shown on top of Fig. 1, there is a constant offset between r_{ij} and r_{ji}. This offset can be estimated and removed from the observations to assure y_l is zero-mean Gaussian. Lastly, half-duplex nature of the PHY layer means that the link cannot be measured simultaneously in both directions which introduces a small time difference between the measurements. As shown on top of Fig. 1, the signal strength has a strong correlation in both directions since $t_a - t_b$ is in the order of milliseconds and the channel gain is almost identical for every k. Thus, $y_l(k)$

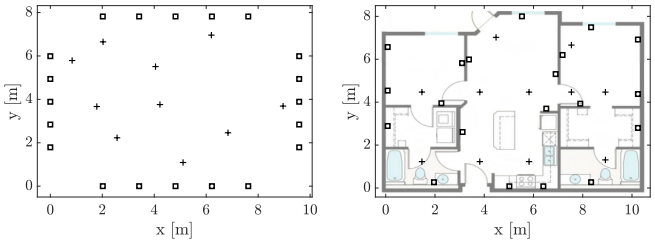

Fig. 2: The experimental layouts in which the nodes (□) and the reference positions (+) are illustrated.

reflects changes in the channel gain if $y_l(k) \sim \mathcal{N}(0, \sigma_{l,0})$. This is an indication that the channel gain is changing rapidly which can be associated to movement of a person as shown in the middle of Fig. 1. Using $y_l(k)$ as input, the energy detector calculates the square sum of L links and movement of the person can be detected as shown on the bottom of Fig. 1.

The reciprocal observation model of the energy detector given in Eq. (8) requires compensating for the offset, μ_l, so that y_l is zero-mean Gaussian. In addition, variance of each link and in the two states is required by EDUV. The maximum likelihood estimates of the parameters are given by

$$\begin{aligned} \hat{\mu}_l &= \tfrac{1}{K} \textstyle\sum_{k=1}^{K} \Delta r_l(k), \\ \hat{\sigma}^2_{l,i} &= \tfrac{1}{K_i} \textstyle\sum_{k=1}^{K} \left(\Delta r_{l,i}(k) - \hat{\mu}_l\right)^2, \end{aligned} \tag{9}$$

where $\Delta \mathbf{r}_{l,i}$ is the subset of measurements for which H_i is true and K_i is the number of measurements in that subset. Batch estimation and supervised training is used for simplicity because focus of this paper is not on parameter estimation. We are solely interested in the reciprocal observation model and performance of the energy detector.

4. EXPERIMENTS

The reciprocal observation model and energy detector are validated using Texas Instruments CC2531 USB dongle nodes [19] that operate on the 2.4 GHz ISM band. The nodes communicate in a round-robin fashion in which one node transmits at a time and the other nodes are in reception mode. The nodes transmit sequentially and a communication cycle, which defines $\mathcal{T}$ of the reciprocal model, consists of one transmission by every node. The nodes communicate on a set of frequency channels $\mathcal{C} \in \{11, \ldots, 26\}$ defined by the IEEE 802.15.4 standard [20]. The channel is updated at the end of each communication cycle following a predefined list. Once each node has transmitted on every channel, the schedule is restarted from the beginning. A detailed explanation of the communication protocol can be found in [21] and [22].

The experiments are conducted in an open indoor environment and in a downtown residential apartment. In both experiments, 20 nodes are deployed as illustrated in Fig. 2. Length of the communication cycle is $\mathcal{T} = 20\tau \approx 58$ ms, where τ is the transmission interval. The person visits the reference positions one after the other and upon reaching a reference position, they stop, remain stationary for a few seconds, and then walk to the next reference position. The person is carrying a video camera in order to measure the time intervals of no movement and movement as a baseline, and in post-processing, the measurements and video streams are synchronized. The experiments in both environments are conducted with one, four and sixteen channels and each experiment is approximately 9 minutes long. See [22] for more details.

	EDEV	EDUV	BM
P_d [%]	99.65 ± 0.56	98.81 ± 1.43	96.02 ± 6.00
P_f [%]	1.37 ± 0.97	0.15 ± 0.16	4.23 ± 4.44
σ_0^2 [dB^2]	0.29 ± 0.13		2.24 ± 2.94
σ_1^2 [dB^2]	1.14 ± 1.64		6.57 ± 7.63

Table 1: Detector performance summarized by different metrics (mean $\pm$ one sigma).

The presented system is evaluated with respect to a variance-based motion detection system which calculates the sample variance for each transmitter-receiver pair [13]

$$s_{ij} = \tfrac{1}{N-1} \textstyle\sum_{m=0}^{N-1} (r_{ij}(k - m|\mathcal{C}|) - \bar{r}_{ij})^2,$$

where N is the measurement buffer length and $\bar{r}_{ij}$ mean of the buffer. Note that the reciprocal observation model calculates $y_l(k)$ over one communication cycle whereas the variance-based detector defines s_{ij} over $(N-1)|\mathcal{C}|+1$ communication cycles. Since this paper aims at detecting movement with the shortest possible time window, the buffer length is set to $N = 2$. Now, a detector that is equivalent to the variance-based detector can be obtained by defining the observation model as

$$y_l(k) = r_{ij}(k) - r_{ij}(k - |\mathcal{C}|) + n(k)$$

and thereafter, the sufficient statistic is calculated using Eq. (2). The benchmark (BM) system also uses supervised training for estimating the variance of each link.

5. RESULTS

There are two notable differences in the studied observation models. The BM model captures all changes affecting the signal strength and as a result, the observations are harder to associate to actual human movement. The reciprocal model only captures fast fading since other temporal changes are within coherence time of the channel and they have the same effect in both directions of the reciprocal links. This difference can be observed by examining σ_i^2 values given in Table 1, and as shown, they are notably lower and they deviate less for the proposed model. The results imply that the modeling assumptions of EDEV are reasonable for σ_0^2 but not for σ_1^2. The second notable difference between the systems is the

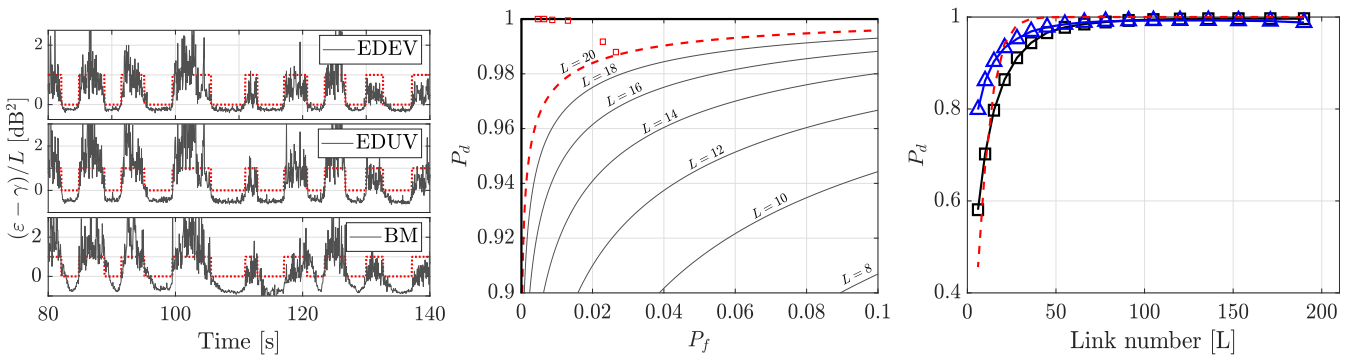

(a) (b) (c)

Fig. 3: In (a), example performance of the energy detectors in the apartment experiment ($|\mathcal{C}| = 16$). In (b), P_f vs. P_d of EDEV (□) and ROC in increments of two $L = [8, 10, \ldots, 18]$ (—), $L = 20$ (- -) and $L = 190$ (—). In (c), probability of detection as a function of link number: ROC (- -), EDEV (-□-) and EDUV (-△-).

observation time window $\mathcal{T}$. It is constant with the reciprocal model, whereas with the BM model it depends on the number of used channels, $\mathcal{T} = 20\tau(|\mathcal{C}| + 1)$. This causes an undesirable delay in the detector output when multiple channels are used as shown in Fig. 3a. The detection probability with the BM model is as low as 84% using $|\mathcal{C}| = 16$ and $P_d > 99\%$ when $|\mathcal{C}| = 1$. This implies that a short observation window is a strict requirement of accurate movement detection. The discussed differences are in favor of the reciprocal observation model and the detection performance is better and more consistent than with the benchmark model.

In the following, performance of EDEV is evaluated using the receiver operating characteristic (ROC) which is defined by σ_0^2, σ_1^2 and L. In the evaluation, $\sigma_0^2 = 0.29$ and $\sigma_1^2 = 1.14$ are fixed while L is varied. It is to be noted that as the ratio σ_1^2/σ_0^2 increases, the detection performance improves and vice versa. The resulting ROC curves are illustrated in Fig. 3b together with the experimental P_f and P_d values for every experiment. As shown in the figure, performance of the detector improves notably as L increases and already with $L = 20$, $P_d = 0.99$ and $P_f < 0.04$. Interestingly, the experimental results lie between the curves of $L = [20,\ 190]$. The signal strength changes are a function of the person's location, movement direction and transceiver positions [2], and if the person is far away from the link the signal strength can remain constant even though the person moves. Thus, the experimental results imply that there are on average 20 links or more that detect movement since the results are above this ROC curve.

The number of nodes, n, has a direct relationship to the cost and the deployment complexity of the system and therefore, it is important to investigate detection performance as a function of n. In the analysis, nodes are removed virtually by discarding their data and this is done in two steps. 1) The data from each node is removed one at a time and the probability of error, $P_e = \frac{1}{2}(P_f + (1 - P_d))$, is calculated. 2) Data of the node that minimizes P_e is permanently removed and thereafter, the procedure goes back to step 1. P_d as a function of $L = n(n-1)/2$ is illustrated in Fig. 3c in which the ROC is calculated using $\sigma_0^2 = 0.29$, $\sigma_1^2 = 1.14$ and $P_f = 0.001$. The ROC and EDEV assume the measurements in each state are i.i.d., which is a reasonable assumption in H_0 but not H_1. EDUV improves the detector performance when $L < 50$ since the model is more accurate. However, the improvement with respect to EDEV diminishes as L grows. Despite modeling inaccuracies, the ROC can be used as a pre-deployment predictor of detection performance, providing an analytical method for system design and pre-deployment performance evaluation. If the design criteria of the system would be $P_f = 0.001$ and it is desired that $P_d > 0.9$, the ROC predicts seven or more nodes are required. The wanted performance is achieved using EDUV and six nodes or EDEV and eight nodes. It is worth noting that L and $\mathcal{T}$ have been fixed in the preceding analysis. The detection performance could be improved by using sequential detection [16, sec. 5.6] or by combining multiple successive communication cycles which increases L.

6. CONCLUSIONS

In this paper, a reciprocal signal strength model is presented, and an energy detector is developed for estimating time periods when a person is moving and stationary. The proposed model minimizes the observation time window and it is shown that this is a strict requirement of accurate movement detection. The experimental results also imply that the model parameters in the stationary state are known, which alleviates the system from time consuming training periods. This streamlines the deployment requirements since the decision threshold can be computed in advance. The developed detector along with the reciprocal model enables low-cost and fast movement detection, which is a significant improvement to the available solutions.

7. REFERENCES

[1] K. Woyach, D. Puccinelli, and M. Haenggi, "Sensorless sensing in wireless networks: Implementation and measurements," in *2006 4th International Symposium on Modeling and Optimization in Mobile, Ad Hoc and Wireless Networks*, 2006, pp. 1–8.

[2] H. Yiğitler, O. Kaltiokallio, R. Hostettler, A. S. Abrar, R. Jäntti, N. Patwari, and S. Särkkä, "RSS models for respiration rate monitoring," *IEEE Transactions on Mobile Computing*, vol. 19, no. 3, pp. 680–696, 2020.

[3] C. Xu, B. Firner, R. S. Moore, Y. Zhang, W. Trappe, R. Howard, F. Zhang, and N. An, "SCPL: indoor device-free multi-subject counting and localization using radio signal strength," in *2013 ACM/IEEE International Conference on Information Processing in Sensor Networks*, 2013, pp. 79–90.

[4] N. Patwari, L. Brewer, Q. Tate, O. Kaltiokallio, and M. Bocca, "Breathfinding: a wireless network that monitors and locates breathing in a home," *IEEE Journal of Selected Topics in Signal Processing*, vol. 8, no. 1, pp. 30–42, 2014.

[5] S. Depatla, A. Muralidharan, and Y. Mostofi, "Occupancy estimation using only WiFi power measurements," *IEEE Journal on Selected Areas in Communications*, vol. 33, no. 7, pp. 1381–1393, 2015.

[6] S. Denis, B. Bellekens, M. Weyn, and R. Berkvens, "Sensing thousands of visitors using radio frequency," *IEEE Systems Journal*, pp. 1–4, 2020.

[7] M. Youssef, M. Mah, and A. Agrawala, "Challenges: device-free passive localization for wireless environments," in *Proceedings of the 13th Annual ACM International Conference on Mobile Computing and Networking*, 2007, p. 222–229.

[8] A. E. Kosba, A. Saeed, and M. Youssef, "RASID: a robust WLAN device-free passive motion detection system," in *2013 IEEE International Conference on Pervasive Computing and Communications*, 2012, pp. 180–189.

[9] P. Hillyard, A. Luong, and N. Patwari, "Highly reliable signal strength-based boundary crossing localization in outdoor time-varying environments," in *2016 15th ACM/IEEE International Conference on Information Processing in Sensor Networks*, 2016, pp. 1–12.

[10] Y. Zheng and A. Men, "Through-wall tracking with radio tomography networks using foreground detection," in *2012 IEEE Wireless Communications and Networking Conference*, 2012, pp. 3278–3283.

[11] A. Al-Husseiny and N. Patwari, "Unsupervised learning of signal strength models for device-free localization," in *2019 IEEE 20th International Symposium on "A World of Wireless, Mobile and Multimedia Networks"*, 2019, pp. 1–9.

[12] P. Hillyard and N. Patwari, "Never use labels: signal strength-based Bayesian device-free localization in changing environments," *IEEE Transactions on Mobile Computing*, vol. 19, no. 4, pp. 894–906, 2020.

[13] J. Wilson and N. Patwari, "See-through walls: motion tracking using variance-based radio tomography networks," *IEEE Transactions on Mobile Computing*, vol. 10, no. 5, pp. 612–621, 2011.

[14] O. Kaltiokallio and M. Bocca, "Real-time intrusion detection and tracking in indoor environment through distributed RSSI processing," in *2011 IEEE 17th International Conference on Embedded and Real-Time Computing Systems and Applications*, 2011, pp. 61–70.

[15] Y. Zhao and N. Patwari, "Robust estimators for variance-based device-free localization and tracking," *IEEE Transactions on Mobile Computing*, vol. 14, no. 10, pp. 2116–2129, 2015.

[16] M. Barkat, *Signal Detection and Estimation*, Artech House, 2005.

[17] J. G. Proakis and M. Salehi, *Digital Communications, 5th ed.*, McGraw-Hill, 2008.

[18] M. Abramowitz and I. A. Stegun, *Handbook of mathematical functions: with formulas, graphs, and mathematical tables*, Dover Publications, 1970.

[19] Texas Instruments, *A USB-enabled system-on-chip solution for 2.4 GHz IEEE 802.15.4 and ZigBee applications*, June 2010, http://www.ti.com/lit/ds/symlink/cc2531.pdf.

[20] IEEE, *IEEE 802.15.4-2003 standard*, October 2003, http://www.ieee802.org/15/pub/TG4Expert.html.

[21] Maurizio Bocca, Ossi Kaltiokallio, and Neal Patwari, "Radio tomographic imaging for ambient assisted living," in *Evaluating AAL Systems Through Competitive Benchmarking*, Stefano Chessa and Stefan Knauth, Eds., Berlin, Heidelberg, 2013, pp. 108–130, Springer Berlin Heidelberg.

[22] O. Kaltiokallio, R. Hostettler, and N. Patwari, "A novel Bayesian filter for RSS-based device-free localization and tracking," *IEEE Transactions on Mobile Computing*, 11 Dec. 2019, Early access.